Austral ECOLOGY A Journal of ecology in the Southern Hemisphere

Austral Ecology (2014) **39**, 158–169

Patterns and drivers of *Araucaria araucana* forest growth along a biophysical gradient in the northern Patagonian Andes: Linking tree rings with satellite observations of soil moisture

ARIEL A. MUÑOZ,[1,2,3]* JONATHAN BARICHIVICH,[6] DUNCAN A. CHRISTIE,[2,5] WOUTER DORIGO,[7] DAVID SAUCHYN,[8] ÁLVARO GONZÁLEZ-REYES,[2,4] RICARDO VILLALBA,[9] ANTONIO LARA,[2,5] NATALIA RIQUELME[2] AND MAURO E. GONZÁLEZ[2,5]

[1]*Centro de Tecnologías Ambientales, Universidad Técnica Federico Santa María, Valparaíso,* [2]*Laboratorio de Dendrocronología y Cambio Global, Instituto de Conservación Biodiversidad y Territorio, Facultad de Ciencias Forestales y Recursos Naturales, Universidad Austral de Chile, Valdivia 5090000, Chile (Email: arimunoz82@gmail.com),* [3]*Centro de Estudios Ambientales (CEAM), Universidad Austral de Chile, Valdivia,* [4]*Departamento de Geología, Facultad de Ciencias Físicas y Matemáticas, Universidad de Chile, Santiago,* [5]*Center for Climate and Resilience Research [CR]2, Chile;* [6]*Climatic Research Unit (CRU), School of Environmental Sciences, University of East Anglia, Norwich, UK;* [7]*Institute of Photogrammetry and Remote Sensing, Vienna University of Technology, Vienna, Austria;* [8]*Prairie Adaptation Research Collaborative (PARC), University of Regina, Regina, Canada; and* [9]*Instituto Argentino de Nivología, Glaciología y Ciencias Ambientales (IANIGLA), CONICET, Mendoza, Argentina*

Abstract *Araucaria araucana* (Araucaria) is a long-lived conifer growing along a sharp west–east biophysical gradient in the Patagonian Andes. The patterns and climate drivers of Araucaria growth have typically been documented on the driest part of the gradient relying on correlations with meteorological records, but the lack of *in situ* soil moisture observations has precluded an assessment of the growth responses to soil moisture variability. Here, we use a network of 21 tree-ring width chronologies to investigate the spatiotemporal patterns of tree growth through the entire gradient and evaluate their linkages with regional climate and satellite-observed surface soil moisture variability. We found that temporal variations in tree growth are remarkably similar throughout the gradient and largely driven by soil moisture variability. The regional spatiotemporal pattern of tree growth was positively correlated with precipitation ($r = 0.35$ for January 1920–1974; $P < 0.01$) and predominantly negatively correlated with temperature ($r = -0.38$ for January–March 1920–1974; $P < 0.01$) during the previous growing season. These correlations suggest a temporally lagged growth response to summer moisture that could be associated with known physiological carry-over processes in conifers and to a response to moisture variability at deeper layers of the rooting zone. Notably, satellite observations revealed a previously unobserved response of Araucaria growth to summer surface soil moisture during the current rather than the previous growing season ($r = 0.65$ for 1979–2000; $P < 0.05$). This new response has a large spatial footprint across the mid-latitudes of the South American continent (35°–45°S) and highlights the potential of Araucaria tree rings for palaeoclimatic applications. The strong moisture constraint on tree growth revealed by satellite observations suggests that projected summer drying during the coming decades may result in regional growth declines in Araucaria forests and other water-limited ecosystems in the Patagonian Andes.

Key words: drought, Patagonia, remote sensing, soil moisture, tree-ring.

INTRODUCTION

The study of forest growth along ecological gradients allows identifying spatial and temporal changes in climatic constraints to plant productivity in relation to the ecological amplitude of the species (Fritts *et al.* 1965; Huang *et al.* 2010; Babst *et al.* 2013). This empirical information is critical to test the parameterization of vegetation models and to estimate the range of responses of forest ecosystems to the ongoing anthropogenic climate change. *Araucaria araucana* (Araucaria) is a long-lived conifer growing along a steep biophysical gradient in the Patagonian Andes of south-central Chile and Argentina (Fig. 1). The relatively small geographic range of the species is constrained by complex topographic, climate and vegetation gradients oriented west–east across the

*Corresponding author.
Accepted for publication April 2013.

doi:10.1111/aec.12054

Andes (Kitzberger 2012), with a strong rain shadow effect and reduction in plant productivity on the eastern side of the continental divide (Fig. 2A,B). As a result, the species occurs in a range of environments varying from dry Mediterranean ecosystems on the western side of the Andes to the altitudinal tree-line and the semiarid Patagonian steppe on the eastern slope of the Andes (Veblen *et al.* 1995).

Fig. 1. Ancient *Araucaria araucana* tress growing on a rocky slope in the North Patagonian Andes.

This region of the South American continent has undergone rapid warming and a general reduction in precipitation during recent decades that together have led to an upward migration of the snowline and a sustained glacial retreat (Carrasco *et al.* 2008; Garreaud *et al.* 2008; Masiokas *et al.* 2008; Garreaud 2009a). Regional climate reconstructions based on tree rings have shown that some of these climate trends are anomalous in the context of the past few centuries (Villalba *et al.* 1998, 2003; Lara *et al.* 2008; Christie *et al.* 2010). Regional climate projections for the coming decades (Garreaud 2009b) suggest further warming and precipitation reduction across the region that will likely result in significant changes in ecosystem functioning and regional hydrology.

The impacts of recent climate change on northern Patagonian forest ecosystems have already been documented for a range of species (Villalba *et al.* 2005, 2012; Veblen *et al.* 2008; Kitzberger 2012). Tree-ring studies have shown a diversity of growth responses across the ecological range of several tree species that are common in the region such as the southern beech *Nothofagus pumilio* (Lara *et al.* 2001, 2005), the xeric conifer *Austrocedrus chilensis* (Villalba & Veblen 1997; LeQuesne *et al.* 2000), and the giant conifer *Fitzroya cupressoides* (Lara *et al.* 2000). Unlike these species, the growth patterns and climate responses of Araucaria

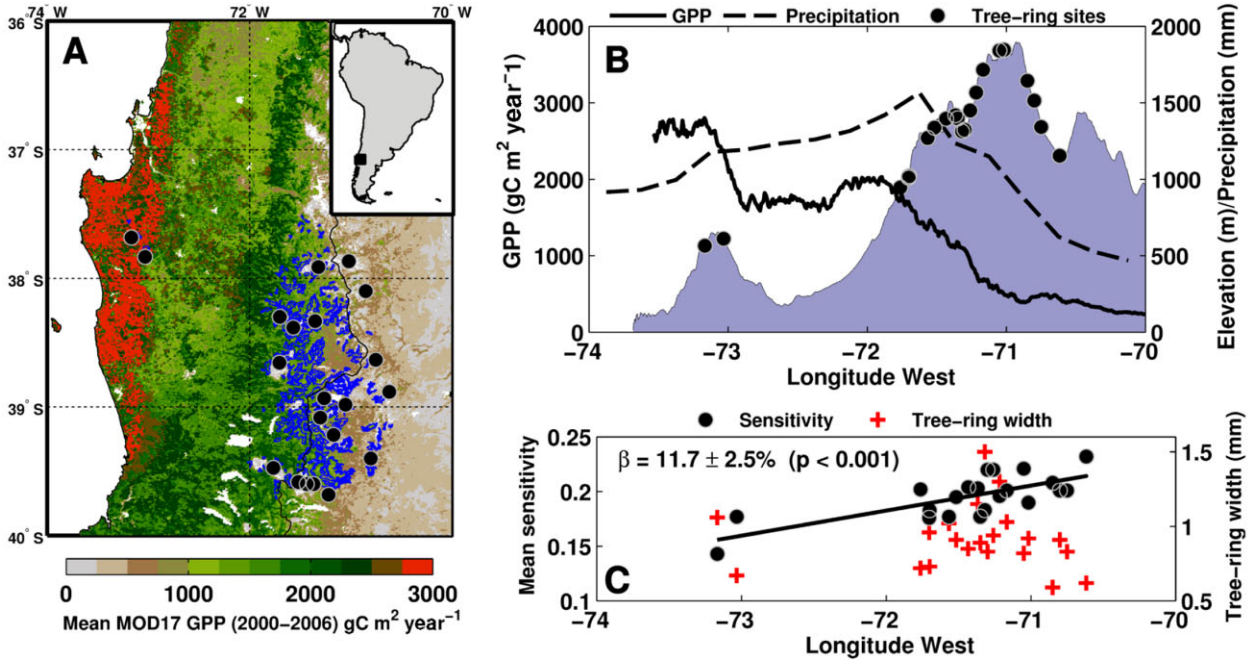

Fig. 2. Location of the Araucaria forests along the biophysical gradient in the North Patagonian Andes of Chile and Argentina. (A) Modern distribution of Araucaria forests (blue) and sampling sites (black points) in a regional landscape of vegetation Gross Primary Productivity (GPP) based on the MOD17 product. (B) West-to-east variation in elevation (grey shading), annual precipitation (dotted line) and annual GPP (bold line). (C) Longitudinal variation in the mean sensitivity statistic (black) and mean tree-ring width (red). The black line represents a significant trend in mean sensitivity along the gradient, expressed as percentage of the overall mean across sites.

doi:10.1111/aec.12054

have not been systematically analysed along its entire ecological range. Significant differences in growth variations and climate constraints would be expected to occur along the dramatic biophysical gradients that shape the geographical range of the species. Most previous tree-ring studies on Araucaria have been focused almost exclusively on the xeric forests growing on the eastern side of the Andes in northern Patagonia (Holmes *et al.* 1979; Veblen *et al.* 1995; Villalba 2000; Mundo *et al.* 2011). These studies have reported a strong synchronism in the growth of the species across this water-limited region linked to regional moisture variability during the previous and current growing seasons, as indicated by a negative correlation with temperature and a positive correlation with precipitation (Veblen *et al.* 1995; Mundo *et al.* 2011), Palmer Drought Severity Index (PDSI; Mundo *et al.* 2011) and streamflow (Holmes *et al.* 1979; Mundo *et al.* 2012). Some small differences in growth patterns and climate response have been observed between high- and low-elevation forests (Mundo *et al.* 2011).

In contrast to the northern Patagonian forests, little is known about the growth dynamics and climate sensitivity of the species in the wetter and more productive forests growing in the western side of the Andes (Veblen *et al.* 1995; González & Veblen 2006). The lack of long-term *in situ* soil moisture observations in the region and in the Southern Hemisphere in general (Dorigo *et al.* 2011) has precluded a direct analysis of the response of austral forests to soil moisture variability. Growth responses of Andean trees to regional moisture variability have instead been assessed indirectly by correlations with local or gridded temperature and precipitation data or with coarsely gridded soil moisture proxies derived from meteorological observations such as the PDSI (Le-Quesne *et al.* 2009; Christie *et al.* 2010; Mundo *et al.* 2012). The recent analysis and development of satellite surface soil moisture products with global coverage and daily resolution based on active and passive microwave observations since the late 1970s (Liu *et al.* 2012) has opened a new avenue for the analysis of the responses of vegetation and terrestrial ecosystems to observed moisture variability (e.g. Dorigo *et al.* 2012). In this study, we compile a network of 21 tree-ring width chronologies spread across the entire range of Araucaria on both slopes of the Andes to (i) describe the spatiotemporal patterns of radial growth of the species in function of the environmental gradients and (ii) to assess their correlation with regional climate variations and satellite observations of surface soil moisture. This work has a larger geographical coverage than previous studies and provides a novel and more comprehensive characterization of the patterns and drivers of Araucaria growth based upon satellite and meteorological observations. Our findings have important implications for palaeoclimatic applications and the understanding of the likely responses of this austral conifer to ongoing climate change.

METHODS

Study region

Araucaria forests occur at mid to high elevations (500–2000 m) along a narrow latitudinal band of the North Patagonian Andes from 37.2°S to 40.2°S (Fig. 2A). Disjoint relict populations also occur in the mountaintops of the Coastal Range of Chile (Villagran 2001), westward of the main range of the species in the Andes. The climate of western side of the Andes (Chile) is temperate with a Mediterranean-like summer drought that ameliorates toward the south, where the climate becomes cooler and wetter. On the eastern side of the Andes (Argentina), the climate becomes more continental with a larger seasonal temperature range and a steady rainfall decrease toward the east because of the rain shadow effect of the Andes, which leads to the forest-steppe ecotone that characterizes Patagonia (Veblen *et al.* 1995; Kitzberger 2012). As a result of the steep topographic gradient, the regional climate varies more with longitude than with latitude. Annual precipitation ranges from 2000 to 3000 mm on the western slope of the Andes to about 500 mm in the Patagonian steppe east of the Andean peaks (Fig. 2B). Vegetation productivity mirrors this precipitation gradient, with a significant eastward decline in model-based gross primary productivity (GPP; Zhao *et al.* 2005) from around 2800 gC m^2 $year^{-1}$ in the productive deciduous broadleaved forests dominated by *Nothofagus* species in the Coastal Range of Chile to about 100 gC m^2 $year^{-1}$ in the Patagonian steppe (Fig. 2A,B).

Tree-ring data

We compiled 21 tree-ring width chronologies of Araucaria covering most of the ecological range of the species in Chile and Argentina (Fig. 2A). Table 1 shows the location and descriptive statistics of each site tree-ring standard chronology, typically based on tree-ring widths from 20 to 30 living overstorey trees and two cores per tree (see Appendix S1(1)).

Mean tree-ring chronologies for each site were developed following standard dendrochronological procedures (see Appendix S1(2)). The Expressed Population Signal statistic (EPS; Briffa 1995) was used to assess the strength of the common growth signal over time and truncate the chronologies when this signal weakens in the less replicated, earlier part of the chronologies (see Appendix S1(3)). The segment of the chronologies with EPS above the commonly used threshold of 0.85 (85% common growth signal and 15% noise) was retained for analysis (Table 1). Accounting for EPS and the time-span of the chronologies, the optimal common period for analysis was 1750–1974. The mean sensitivity statistic (Fritts 1976) was used to evaluate the degree of sensitivity of year-to-year variability of tree growth to environmental variation at each site and to identify geographic differences of tree growth dynamics (see Appendix S1(4)).

doi:10.1111/aec.12054

Table 1. Location and statistics of the tree-ring width chronologies of *Araucaria araucana* used in this study

Code	Name[†]	Lat. (S)	Long. (W)	Elev. (m a.s.l.)	*n*[‡]	Period	EPS[§]	r[¶]	TRW[††]	MS[‡‡]
CAR	Caramávida (cl)	37°41′	73°10′	900	22	1474–1975	1750	0.61	1.06	0.14
PAG	Piedra del Águila (cl)	37°50′	73°02′	1300	51	1239–2009	1450	0.49	0.67	0.17
QUE	Quetrupillán (cl)	39°47′	71°76′	1310	25	1483–2005	1630	0.49	0.72	0.20
CAP	Captrén (cl)	38°39′	71°42′	1492	51	1664–2007	1720	0.54	0.96	0.17
TOL	Tolhuaca (cl)	38°17′	71°42′	1280	29	1608–2002	1750	0.45	0.73	0.18
LON	Lonquimay (cl)	38°23′	71°34′	1510	56	1664–1975	1720	0.56	1.02	0.17
LAN	Lanín (cl)	39°35′	71°30′	1350	95	1585–2000	1715	0.45	0.91	0.19
PAT	Paso Tromen (ar)	39°36′	71°26′	1350	22	1385–1983	1740	0.53	0.85	0.20
LAT	LagoTromen (ar)	39°36′	71°22′	1010	54	1617–1986	1670	0.58	1.15	0.20
NAL	Las Nalcas (cl)	38°20′	71°21′	1420	31	1375–1975	1590	0.53	0.89	0.17
VIZ	Vizcacha (cl)	37°54′	71°19′	1323	24	1673–2006	1805	0.41	1.5	0.18
ESP	Estancia Pulmari (ar)	39°05′	71°18′	1890	28	1589–1989	1650	0.62	0.83	0.23
LAM	Lago Moquehue (ar)	38°93′	71°26′	710	13	1665–1974	1750	0.58	0.94	0.22
ESM	E.MaluilMalal (ar)	39°41′	71°13′	890	29	1689–1976	1750	0.55	1.3	0.19
LAR	LagoRucachoroy (ar)	39°13′	71°10′	1330	47	1377–1976	1510	0.56	1.03	0.20
LOL	Lonco Luan (ar)	38°59′	71°03′	1110	51	1306–1974	1420	0.52	0.82	0.22
CAV	Caviahue (ar)	37°52′	71°01′	1545	28	1444–1974	1660	0.52	0.92	0.19
CHE	ChenquePehuen (ar)	38°06′	70°51′	1650	44	1246–1974	1490	0.56	0.59	0.21
RAH	Rahue (ar)	39°24′	70°48′	1380	26	1483–1974	1540	0.58	0.91	0.20
PIH	PinoHachado (ar)	38°38′	70°45′	1400	31	1459–1974	1690	0.56	0.83	0.20
PPA	P. PinosAlumine (ar)	38°53′	70°37′	1610	38	1140–1974	1390	0.56	0.62	0.22

[†]cl = Chile, ar = Argentina. [‡]Number of cores. [§]First year with EPS above 0.85. [¶]Series intercorrelation. [††]Mean tree-ring width measurement (mm). [‡‡]Mean sensitivity. EPS, Expressed Population Signal; MS, mean sensitivity.

Spatiotemporal variability

Empirical Orthogonal Functions (EOF) analysis was used to evaluate the spatiotemporal patterns of tree growth across the tree-ring network. The EOF analysis was based on the correlation matrix of the 21 tree-ring chronologies over the common period from 1750 to 1974. A Monte Carlo significance test (Jolliffe 2002) indicated that only the first two EOFs were significant at the 95% level and thus only these EOFs were retained for further analysis.

Climate drivers of tree growth

Simple and partial correlation analysis as implemented in the seascorr Matlab routine (Meko *et al.* 2011) was used to identify the months and seasons where precipitation and temperature are critical for tree-ring growth within a 26-month period from April of the calendar year prior to growth onset to May of the calendar year following the growth onset, when the austral growing season ends. This extended temporal window allows the identification of potential physiological carry-over effects in tree growth as it spans the previous and current austral growing seasons. Simple correlations between the amplitudes of the first two EOFs of the tree-ring network and gridded total monthly precipitation from the CRUTS 3.2 dataset (Harris *et al.* 2013) averaged over the region 37°50′–40°S and 70°50′–73°50′W were computed for each month over the period 1920–1974. The same was done for mean monthly temperature but using partial correlations in order to remove the potential confounding influence of any correlation between regional temperature and precipitation (Briffa *et al.* 2002). The significance of the correlations and partial correlations was empirically estimated using 1000 Monte Carlo simulations (Meko *et al.* 2011).

In order to examine the direct relationship between the growth of Araucaria and soil moisture, the leading EOFs of the six most up-to-date tree-ring chronologies of the dataset (Table 1) were compared with satellite microwave soil moisture observations from a newly developed global dataset with a spatial resolution of 0.25° and daily time step (Liu *et al.* 2012; available at: http://www.esa-soilmoisture-cci.org/; see Appendix S1(5)). Although these satellite observations only represent moisture in the uppermost few centimetres of the soil profile it has been shown that they correlate well with moisture variations at deeper layers (Albergel *et al.* 2008) and with the self-calibrating Palmer Drought Severity Index (sc-PDSI) based on gridded meteorological observations (van der Schrier *et al.* 2013). More information about this dataset can be found in Appendix S1(6).

RESULTS

Growth patterns

The xeric sites located along the North Patagonian steppe tended to have slower and more variable yearly growth rates than the sites located at high elevations and under more mesic conditions in the Pacific side of the Andes (Fig. 2C, Table 1). The mean sensitivity statistic increased significantly toward the east by about 11.7%

doi:10.1111/aec.12054

($P < 0.001$) per each degree of longitude (Fig. 2C), following the increase in aridity. Unlike gross plant productivity and mean sensitivity, the site-level mean ring width did not follow an overall trend along the longitudinal gradient but it decreased markedly near the North Patagonian steppe (Fig. 2C). However, in spite of these regional differences in the magnitude and variability of the growth rates, the temporal variations of the chronologies are remarkably similar (Fig. 3). This similarity was confirmed by a high degree of intercorrelation between the chronologies over the common period 1750–1974 (Appendix S2), suggesting that there is a strong regional signal in year-to-year variations in the growth of Araucaria along the west-to-east environmental gradient.

The first EOF accounted for 44.3% of the total variance of the tree-ring network between 1750 and 1974, with all sites having positive loadings (Fig. 4A,C). Regressing the spatial loadings of this EOF onto latitude, longitude and elevation showed that the magnitude of the loadings varied significantly only with longitude ($r^2 = 0.29$, $P < 0.05$) following an eastward increase. Therefore, this EOF represented a region-wide pattern of common interannual to decadal growth variability with a slight dominance by a cluster of sites in the eastern side of the Andes. The temporal variability of the amplitude of this EOF exhibited strong decadal variability and the magnitude of the anomalies has increased substantially since around 1850 as indicated by a strong increase in the overall variance of the time series (Fig. 4A).

The second EOF was marginally significant and explained only 8.1% of the total variance in the dataset (Fig. 4B). This EOF was associated with a secondary spatiotemporal pattern describing a contrast in tree-growth variations between the eastern and western slopes of the Andes, as indicated by negative loadings in the sites located on the Coastal Range of Chile and the Pacific side of the Andes and positive loadings in several but not all sites on the eastern side of the Andes (Fig. 4D). As a result, compared with latitude ($r^2 = 0.16$, $P > 0.05$) and elevation ($r^2 = 0.03$, $P > 0.05$), longitude ($r^2 = 0.30$, $P < 0.001$) explained most of the variability in the spatial pattern of the EOF loadings. Unlike the first EOF, this spatiotemporal pattern of tree growth did not show a large change in overall variance through time, although there is still a slight increase (Fig. 4B). Overall, the EOF analysis indicated a dominant region-wide synchrony in interannual to decadal tree-growth variations with some small differences occurring along the longitudinal gradient imposed by the Andes.

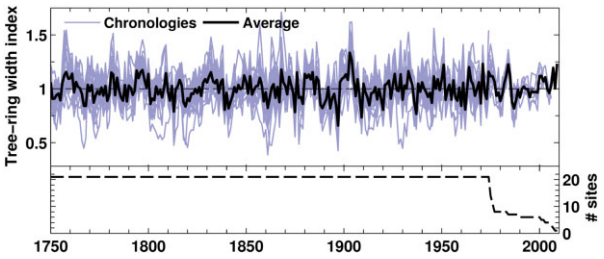

Fig. 3. Time series of the individual tree-ring chronologies of Araucaria (grey) together with their average (black) and number of sites through time.

Tree-ring growth and regional climate

Simple and partial correlations between the individual chronologies and the regional series of precipitation

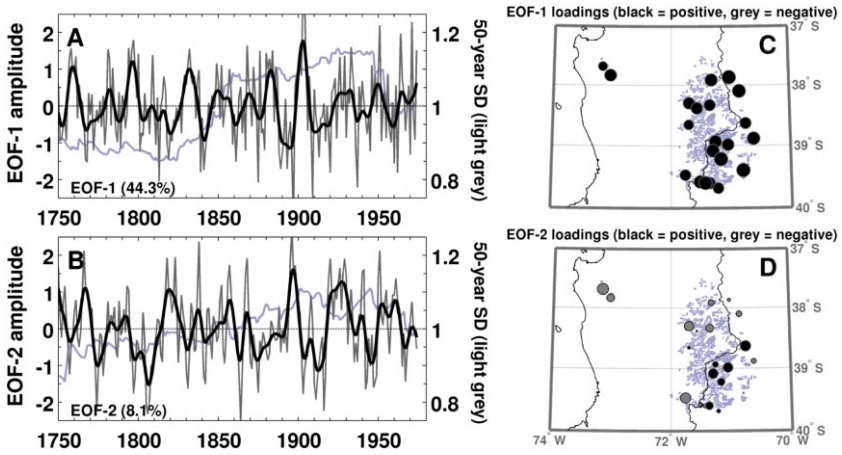

Fig. 4. Temporal and spatial patterns of the (A, C) first and (B, D) second Empirical Orthogonal Function (EOF) of the tree-ring network from 1750 to 1974. A 10-year cubic smoothing spline (bold line) is used to show decadal variations in the amplitude of the EOFs whilst changes in variance through time are shown by a simple 50-year sliding standard deviation (light grey). The size of the markers in the maps is proportional to the magnitude of the EOF loading of each site and the grey shading represents the distribution of Araucaria forests.

doi:10.1111/aec.12054

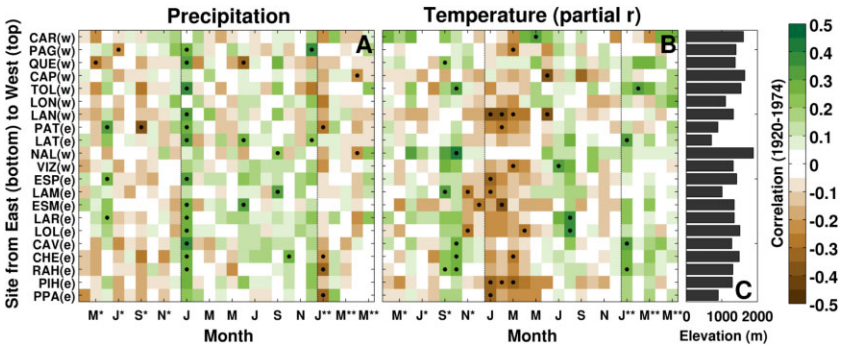

Fig. 5. Correlation between each tree-ring chronology in the network and regionally averaged (A) total monthly precipitation and (B) mean monthly temperature from 1920 to 1974. Correlations are given for a 26-month window from April of the previous calendar year (*) to May of the following year (**). The stippling indicates months with significant correlations ($P < 0.05$). Note that partial correlations are given for temperature and simple correlations for precipitation. The elevation of the chronologies is shown in C and their location east (e) or west (w) of the continental divide is given next to the site name.

and temperature highlight the well-known association of Araucaria tree rings with meteorological conditions during the previous growing season, with a general pattern of positive and significant correlations with precipitation ($r = 0.24$ to 0.37, $P < 0.05$) and negative correlations with temperature (partial $r = -0.26$ to -0.38, $P < 0.05$) across most of the sites (Fig. 5). Thirteen out of 21 chronologies located on both sides of the Andes showed a dominant significant correlation with precipitation during January of the previous growing season (Fig. 5A), when rainfall reaches the seasonal minimum and temperatures rise near the seasonal peak (Appendix S1(7)).

Negative partial correlations with temperature were largely restricted to the drier second part of the previous growing season from January to May (Fig. 5B). However, their timing, magnitude and significance varied substantially across sites and only 11 chronologies had at least 1 month with a significant correlation during this period. Most of these chronologies are located on the eastern side of the Andes, indicating that this negative relationship with temperature tends to be more common toward the drier end of the gradient (Appendix S4B). Indeed, the magnitude of the negative correlations in February increases significantly with longitude toward the east ($r^2 = 0.26$, $P < 0.01$). The pattern of negative correlations with summer temperatures in these sites contrasted with a group of seven sites having significant and positive correlations with early spring (September–October) temperatures at the start of the previous growing season (Fig. 5B), when low temperatures typically limit tree-ring growth. These sites tended to have a relatively weaker negative correlation with summer temperatures. Regressing the partial correlation during October onto elevation indicated that this positive association was not related to differences in elevation ($r^2 = 0.10$, $P > 0.05$). Similar correlation patterns between tree rings and monthly temperature are obtained when using simple instead of partial correlations (Appendix S3B).

The association of Araucaria tree-ring growth with meteorological conditions during the current growing season was relatively weak and no clear common patterns emerged (Fig. 5). A few chronologies had significant and positive correlations with temperature ($r = 0.26$ to 0.35, $P < 0.05$) and negative correlations with precipitation ($r = -0.29$ to -0.32, $P < 0.05$) in January of the current growing season. This emphasizes the importance of the temporally lagged response of Araucaria tree-ring growth to climate variability.

The dominant patterns of correlation with regional temperature and precipitation described for the individual tree-ring chronologies above are summarized well by the correlation between the amplitude of the first two EOFs of the tree-ring network and these meteorological variables (Fig. 6). The first EOF, representing the common regional tree-ring growth signal, was significantly correlated with precipitation only during January of the previous growing season ($r = 0.35$, $P < 0.05$; Appendix S5B) as seen in most of the sites. The relationship between this EOF and temperature highlights the negative correlation between Araucaria tree-ring growth and summer temperatures during the previous growing season (partial $r = -0.26$ to -0.31, $P < 0.05$; Fig. 6B; see Appendix S1(8)).

The second EOF, representing a secondary pattern of east–west contrast on tree-ring growth variations along the longitudinal environmental gradient, was more strongly correlated with temperatures than with precipitation on a month-to-month basis (Fig. 6C,D). This EOF was not significantly correlated with precipitation during any individual month, however, a significant and positive relationship appeared when precipitation was aggregated from November to January during the current growing season ($r = 0.32$,

doi:10.1111/aec.12054

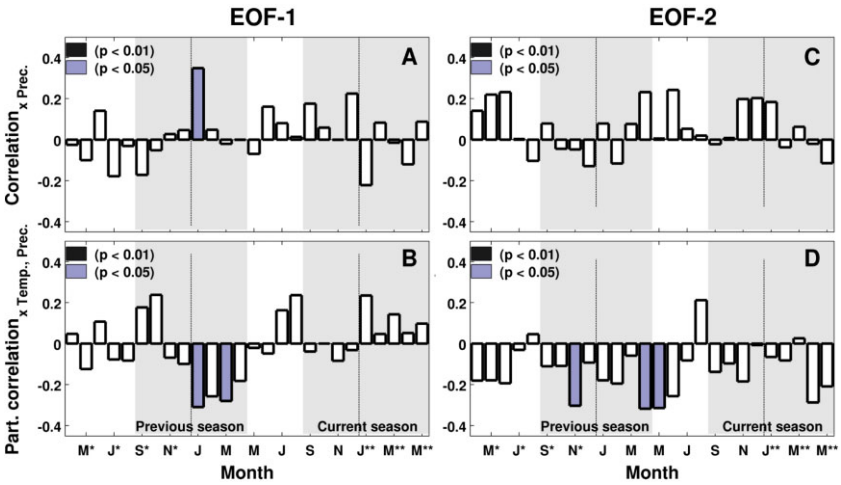

Fig. 6. Correlation between the amplitude of the first two Empirical Orthogonal Functions (EOFs) of the tree-ring network and regional series of (A, C) monthly precipitation and (B, D) temperature from 1920 to 1974. Correlations are given for a period of 26 months starting in April of the previous calendar year and ending in May of the following calendar year. Note that partial correlations are used for temperature. The vertical lines separate months of the previous (*), current, and following (**) calendar years with respect to the start of tree growth in the austral spring.

$P < 0.05$; Appendix S5D). Like the first EOF, this secondary mode of tree growth was also negatively correlated with temperatures during the previous growing season but the association was stronger and significant around the start (November; partial $r = -0.30$, $P < 0.05$) and end (April–May; partial $r = -0.38$, $P < 0.01$; Appendix S5C) of the growing season rather than at the summer peak (Fig. 6D). Also, the nearly significant positive relationship with late winter-spring temperatures was weaker than in the first EOF and restricted to August of the current growing season (partial $r = 0.20$, $P > 0.05$; Fig. 6D). This temperature signal in August was significant in two sites (LAR and LOL) located in the eastern side of the Andes (Fig. 5B; See Appendix S1(9)).

Tree-ring growth and surface soil moisture

The first EOF of the six chronologies located on the western slope of the Andes that span the period 1750–2000 was used to assess the response of Araucaria tree-ring growth to regional variations in satellite-observed surface soil moisture since 1979. This EOF was highly correlated with the first EOF based on the 21 chronologies over the period 1750–1974 ($r = 0.89$, $P < 0.01$; Appendix S6); therefore, it captured the regional tree-ring growth signature seen in the entire network. A simple comparison between this EOF and regionally averaged summer (December–February) surface soil moisture during 1979–2000 revealed a remarkable correlation of Araucaria tree-ring growth with soil moisture during the current growing season ($r = 0.65$, $P < 0.05$; Fig. 7A). This summer soil moisture signal during the current growing season has a large and significant spatial footprint across the mid-latitudes of the South American continent from 35°S to 45°S (Fig. 7B).

When comparing each of the six tree-ring chronologies with regional soil moisture on a month-to-month basis during the current and previous warm seasons (October–May), a consistent pattern of significant correlations during most of the current growing season appeared across the sites (Appendix S7). No significant correlations occurred during the previous growing season, in contrast with the correlation patterns observed between tree-ring growth and regional temperature and precipitation (Figs 5 and 6).

In order to understand this contrasting temporal lag in the growth responses based on meteorological and satellite observations, we assessed the temporal memory of summertime surface soil moisture in the region by correlating the regional series of satellite-observed summer soil moisture with regionally averaged monthly precipitation and temperature over a range of months prior to the austral summer. We found that the regional series of summer surface soil moisture averaged between December and February started to be consistently and positively correlated with regional precipitation only since late-winter/early-spring (August; Appendix S8), immediately following the peak of the rainy season in the region. Similarly, summer averaged soil moisture was consistently and negatively correlated with regional temperatures only during February (Appendix S8), when temperatures reach the seasonal peak and thereby become an

doi:10.1111/aec.12054

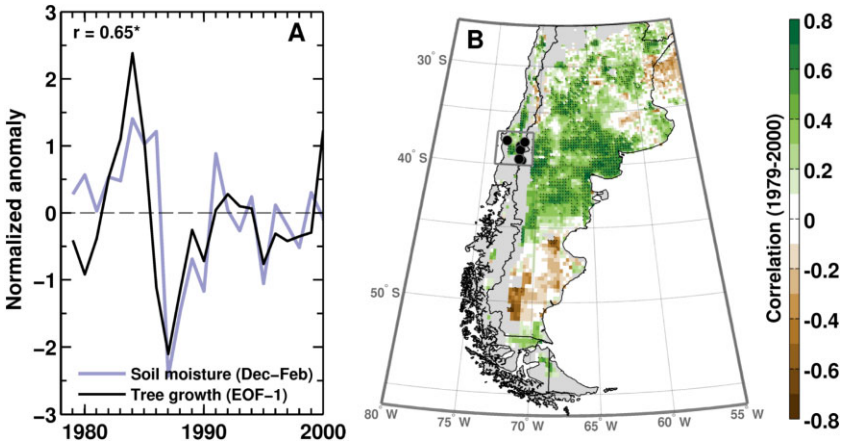

Fig. 7. Comparison of the leading Empirical Orthogonal Function (EOF) of six updated tree-ring chronologies of Araucaria with (A) regional satellite-observed summer (Dec–Feb) soil moisture and (B) correlation field between this EOF and summer soil moisture variability across southern South America from 1979 to 2000. The black dots in the map indicate the locations of the tree-ring chronologies and the grey rectangle denotes the region used to average soil moisture in A. The stippling indicates significant correlations ($P < 0.05$). Grid-boxes with less than 15 years of soil moisture data were excluded from correlation analysis and are indicated by grey shading.

important driver of evapotranspiration. This suggests that summer averaged surface soil moisture integrates meteorological conditions for a period of about 6 months, which extends from the start of the growing season in spring. Therefore, the temporal memory of surface soil moisture is substantially shorter than that of tree rings as suggested by the lagged correlations with the previous growing season meteorological conditions. Notice that snow may only have a very marginal influence if any on our regional series of summer soil moisture, as satellite moisture retrievals are available for lowlands only (see Fig. 7B).

DISCUSSION

Growth patterns

Patterns and climate drivers of the radial growth of temperate tree species in the Southern Andes have typically been found to vary considerably along the major biophysical gradients in the region associated with elevation, latitude and longitude (e.g. Villalba & Veblen 1997; Lara *et al.* 2000, 2001, 2005; LeQuesne *et al.* 2000; Christie *et al.* 2010; Kitzberger 2012). This study shows that despite these gradients, the growth of Araucaria is remarkably synchronous across the study region (Figs 3 and 4), with small but significant differences occurring only along the longitudinal aridity gradient imposed by the Andes. The large degree of growth synchronism compared with other tree species occurring in the region can be explained, in part, by the relatively small latitudinal extent of the geographic range of Araucaria that usually lies under similar synoptic conditions associated with dominant westerly circulation. The influence of Atlantic weather systems in the forests located on the eastern side of the Andes is minimal (Veblen 2007).

A similar degree of common growth variability in the growth of Araucaria was found by Mundo *et al.* (2011) based on a network of 17 tree-ring sites over a reduced domain across the North Patagonian forests. However, their tree-ring network is not totally independent of ours as 11 of their sites are updated versions of earlier collections by LaMarche *et al.* (1979) and Villalba *et al.* (1989) included in our database. The first EOF of their tree-ring network accounted for 62.3% of the total variance over the period 1676–1974, which is higher than the 44.3% of the total variance accounted for by the first EOF of our network of 21 sites over the shorter period 1750–1974 but covering a much larger spatial domain. They also identified a secondary pattern of growth variability along the elevation gradient, associated with the second EOF of their network, but it only accounted for about 7% of the total variance. Unlike this earlier study, we did not identify significant spatial differences in growth patterns along the elevation gradient across the Andes. Instead, on a regional scale, small but significant differences in tree growth occur primarily along the longitudinal aridity gradient generated by the Andes, but accounting only for about 8% of the total variance (Fig. 4B,D).

The dominant regional pattern of Araucaria tree-ring growth identified in our network displayed a long-term increase in the amplitude and frequency of extreme growth events since around the 1850s (Fig. 4A). A similar increase in growth variance

doi:10.1111/aec.12054

through time has been observed in tree rings of the drought-sensitive conifer *Austrocedrus chilensis* north of the study region (Le-Quesne *et al.* 2006; Christie *et al.* 2010) and southern beech (*Nothofagus pumilio*) growing in the forest-steppe ecotone along the Patagonian Andes (Villalba *et al.* 2001). Hence, this seems to be a common feature of tree growth across the region and may be indicating a long-term amplification of the interannual variability of the common climate forcing of tree growth in the mid-latitudes of the South American continent. This could be related to a secular increase in ENSO activity and/or to a strengthening of the ENSO teleconnection in the austral mid-latitude regions as suggested by tree rings of the ENSO-sensitive conifer *Agathis australis* (kauri) in New Zealand (Fowler *et al.* 2012). However, a similar change in variance through time can also arise from the increasing dominance of young, fast-growing trees in the average chronologies toward the present, where the increasing abundance of wider and more highly variable young rings combined with rings from older, slow-growing trees progressively inflates the variance. The identification of the underlying cause of this variability feature is beyond the scope of this paper and should be addressed in a future study.

Climate drivers

Earlier studies have typically found a modest ($r^2 < 0.20$) and temporally lagged response of Araucaria tree rings to climate variability, characterized by a predominantly negative correlation with temperature and a positive correlation with precipitation during most of the previous growing season and to a lesser extent during the current growing season (Veblen *et al.* 1995; Villalba 2000; González & Veblen 2006; Mundo *et al.* 2011). Consistent with these studies, we found a similar pattern of correlations between Araucaria tree-ring growth and regional temperature and precipitation during the previous growing season (Figs 5 and 6), using gridded climate data (Harris *et al.* 2013). It is necessary to consider that the gridded data are interpolations of irregularly distributed instrumental records, resulting in differences in accuracy through time. Futures studies should consider more detailed comparisons with local records.

This pattern of time-lagged correlations with temperature and precipitation has been interpreted in previous studies as an indication for a dominant spring–summer soil moisture control on Araucaria tree-ring growth, which is consistent with a positive correlation of Araucaria tree rings with regional streamflow (Holmes *et al.* 1979; Mundo *et al.* 2012) and coarsely gridded PDSI data (Mundo *et al.* 2011).

The strong association found in this study between the regional pattern of tree-ring growth and summer satellite-observed surface soil moisture over the period 1979–2000 confirms the dominant control of soil moisture content on the growth of Araucaria (Fig. 7). However, in contrast to the time-lagged response pattern indirectly inferred from correlations with meteorological data, the satellite observations show a significant growth response to soil moisture variability only during spring and summer of the current growing season (Appendix S7). Therefore, the satellite observations have revealed a large non-lagged control of soil moisture availability on the growth of Araucaria during the current growing season that has been largely unobserved in previous studies relying on meteorological records. This response explains a large fraction of the remaining growth variance not accounted for by the relatively modest growth response to meteorological conditions during the previous growing season. A similar response pattern to soil moisture availability was observed by Mundo *et al.* (2011) in northern Patagonia, where Araucaria tree rings were significantly correlated with PDSI only during spring and summer of the current growing season.

The contrasting time lag between the growth responses revealed by satellite observations and those inferred from temperature and precipitation data alone may be primarily associated with the different physical nature of the variables and to the underlying mechanisms that link them to tree physiology and cambial growth (Kozlowski & Pallardy 1997; Vaganov *et al.* 2006). For instance, unlike the primary meteorological observations of temperature and precipitation, satellite-sensed surface soil moisture dynamics integrate current and previous meteorological conditions (e.g. precipitation, temperature, radiation and wind) over a range of temporal scales from a few days to several months (Rebel *et al.* 2012). We found that throughout the region, summertime surface soil moisture represents the land surface water balance integrated over a period of about 6 months since the beginning of the precedent spring, when the growing season starts (Appendix S8). This temporal memory in soil moisture dynamics is expected to become longer at deeper layers of the soil profile. Indeed, field observations of late-summer hydrogen and oxygen isotopic composition of soil water content in the region have shown that soil water at greater depths originate from rainfall in the last or even prior to the last rainy seasons rather than from recent rainfall events (Schulze *et al.* 1996). Therefore, we speculate that the lagged correlations with meteorological data could be indicating a growth response to moisture in deeper layers of the rooting zone. In addition, known physiological carry-over processes in the cambial activity of conifers (Vaganov *et al.* 2006) may also contribute to the temporal lag in growth response suggested by the meteorological data.

doi:10.1111/aec.12054

The forthcoming release of a new high-resolution global dataset of self-calibrating PDSI (sc-PDSI) from 1901 to 2009 (van der Schrier *et al*. 2013) based on the meteorological datasets of the Climatic Research Unit will allow a longer-term empirical assessment of the response of Araucaria and other Andean forest ecosystems to regional moisture variations.

Because of the strong common regional signal in the growth of Araucaria associated with a dominant moisture limitation during the growing season, there was only a small degree of spatial variation in the climate response along the environmental gradient across the Andes (Figs 5 and 6). As one would expect, the moisture limitation tends to become stronger toward the driest part of the longitudinal aridity gradient. The strongest negative correlations between the tree-ring chronologies and summer temperatures during the previous growing season occur in northern Patagonia. In this same region, Mundo *et al*. (2011) found a stronger albeit barely significant growth response to spring and summer moisture variability in low-elevation sites compared with higher elevations based on correlations with coarsely gridded PDSI data. Beside these negative correlations, there was also some indication that the regional growth pattern identified across our network is positively correlated with late winter and early spring temperatures (Fig. 6), when cold conditions are the dominant limitation for cambial activity and tree-ring growth in temperate regions (Rossi *et al*. 2006; Vaganov *et al*. 2006). A larger degree of local variability in growth response along the gradient should appear when using local rather than regional series of temperature and precipitation for correlation analysis.

The satellite observations revealed that the spatial footprint of the summer moisture signal embedded in the regional growth of Araucaria extends over most of the mid-latitudes of the South American continent between 35°S and 45°S (Fig. 7B). This result is encouraging for the ongoing efforts to develop a spatially resolved reconstruction of past drought variability in South America based on the continental tree-ring network. However, an urgent update of the available tree-ring data of Araucaria is required in order to fully exploit the large-scale moisture signature recorded by the tree rings of this austral conifer. The pattern of mid-latitude summer drying projected by climate models during the coming decades (Garreaud 2009b) may result in regional growth declines and eventually increased tree mortality rates in Araucaria forests and other water-limited ecosystems in the Patagonian Andes. Some of these projected large-scale trends and associated ecosystem responses may be already taking place (e.g. Jung *et al*. 2010; Zhao & Running 2010; Villalba *et al*. 2012).

ACKNOWLEDGEMENTS

This work was carried out with the aid of grants from the Inter-American Institute for Global Change Research CRN II # 2047 supported by and the US National Science Foundation (GEO-0452325), and the Chilean Research Council (FONDECYT 1120965 and FONDECYT 1121106 and FONDAP 1511009). Much of the tree-ring data for this study was obtained from the International Tree-Ring Data Bank. This study was completed using the facilities of the Prairie Adaptation Research Collaborative at the University of Regina, Canada, where support came from the IDRC sponsored VACEA project. AM and JB were supported by a scholarship from the Chilean Government for doctoral studies under the programme Formación de Capital Humano Avanzado of CONICYT.

REFERENCES

Albergel C., Rüdiger C., Pellarin T. *et al*. (2008) From near-surface to root-zone soil moisture using an exponential filter: an assessment of the method based on in-situ observations and model simulations. *Hydrol. Earth Syst. Sci.* **12,** 1323–37. doi:10.5194/hess-12-1323-2008.

Babst F., Poulter B., Trouet V. *et al*. (2013) Site and species specific responses of forest growth to climate across the European continent. *Glob. Ecol. Biogeogr.* doi: 10.1111/geb.12023.

Briffa K. R. (1995) Interpreting high-resolution proxy climate data: the example of dendroclimatology. In: *Analysis of Climate Variability, Applications of Statistical Techniques* (eds H. von Storch & A. Navarra) pp. 77–94. Springer, Berlin, Heidelberg, New York.

Briffa K. R., Osborn T. J., Schweingruber F. H., Jones P. D., Shiyatov S. G. & Vaganov E. A. (2002) Tree-ring width and density data around the Northern Hemisphere: Part 1, local and regional climate signals. *Holocene* **12,** 737–57.

Carrasco J., Osorio R. & Casassa G. (2008) Secular trend of the equilibrium line altitude in the western side of the southern Andes derived from radiosonde and surface observations. *J. Glaciol.* **54,** 538–50.

Christie D., Boninsegna J. A., Cleavelan M. K. *et al*. (2010) Aridity changes in the Temperate-Mediterranean transition of the Andes since ad 1346 reconstructed from tree-rings. *Clim. Dynam.* **36,** 1505–21.

Dorigo W. A., de Jeu R. A. M., Chung D. *et al*. (2012) Evaluating global trends (1988–2010) in harmonized multi-satellite surface soil moisture, *Geophys. Res. Lett.* doi:10.1029/2012GL052988.

Dorigo W. A., Wagner W., Hohensinn R. *et al*. (2011) The International Soil Moisture Network: a data hosting facility for global in situ soil moisture measurements. *Hydrol. Earth Syst. Sci.* **15,** 1675–98. doi:10.5194/hess-15-1675-2011.

Fowler A., Boswijk G., Lorrey A. *et al*. (2012) Multi-centennial tree-ring record of ENSO-related activity in New Zealand. *Nat. Clim. Change* **2,** 172–6.

Fritts H. C. (1976) *Tree Rings and Climate*. Academic Press, London, New York.

Fritts H. C., Smith D. G., Cardis J. W. & Budelsky C. A. (1965) Tree-ring characteristics along a vegetation gradient in northern Arizona. *Ecology* **46,** 393–401.

Garreaud R. (2009a) The Andes climate and weather. *Adv. Geosci.* **22,** 3–11.

Garreaud R. (2009b) *Climate Variability in Chile: Assessment Interpretation and Proyections. Research Team Grants in Science and Tecnology*. Final Proyect Report. CONICYT, Programa Bicentenario de Ciencia y Tecnología, Unidad de Monitoreo y Evaluación, Providencia.

Garreaud R., Vuille M., Compagnucci R. & Marengo J. (2008) Present-day South American climate. *Palaeogeogr. Palaeoclimatol. Palaeoecol.* **281,** 180–95.

González M. E. & Veblen T. (2006) Climatic influences on fire in *Araucaria araucana – Nothofagus* forests in the Andean cordillera of south-central Chile. *Ecoscience* **13,** 342–50.

Harris I., Jones P. D., Osborn T. J. & Lister D. H. (2013) Updated high-resolution grids of monthly climatic observations. *Int. J. Climatol.* doi: 10.1002/joc.3711.

Holmes R. L., Stockton C. W. & Lamarche V. C. (1979) Extension of river flow records in Argentina from long tree-ring chronologies. *Water Resour. Bull.* **15,** 1081–5.

Huang J., Tardif J. C., Bergeron Y., Denneler B., Berninger F. & Girardin M. P. (2010) Radial growth response of four dominant boreal tree species to climate along a latitudinal gradient in the eastern Canadian boreal forest. *Global Change Biology* **16,** 711–31.

Jolliffe I. T. (2002) *Principal Component Analysis* Springer, New York.

Jung M., Reichstein M., Ciais P. *et al*. (2010) Recent decline in the global land evapotranspiration trend due to limited moisture supply. *Nature* **467,** 951–4. doi:10.1038/nature09396.

Kitzberger T. (2012) Ecotones as complex arenas of disturbance, climate and human impacts: the trans-Andean forest-steppe ecotone of northern Patagonia. In: *Ecotones between Forest and Grassland* (ed. R. Myster) pp. 59–88. Springer, New York. ISBN 978-1-4614-3796-3.

Kozlowski T. T. & Pallardy S. G. (1997) *Growth Control in Woody Plants*. Academic Press, London.

Lara A., Aravena J. C., Villalba R., Wolodarsky-Franke A., Luckman B. & Wilson R. (2001) Dendroclimatology of high-elevation *Nothofagus pumilio* forests at their northern distribution limit in the central Andes of Chile. *Can. J. For. Res.* **31,** 925–36.

Lara A., Villalba R., Aravena J. C., Wolodarsky A. & Neira E. (2000) Desarrollo de una red de cronologías de Fitzroya cupressoides (Alerce) para Chile y Argentina. In: *Dendrocronologia en América Latina* (ed. F. Roig) pp. 217–44. EDIUNC, Mendoza.

Lara A., Villalba R. & Urrutia R. (2008) A 400-year tree-ring record of the Puelo River summer–fall streamflow in the Valdivian Rainforest eco-region, Chile. *Clim. Change* **86,** 331–56.

Lara A., Villalba R., Wolodarsky-Franke A., Aravena J. C., Luckman B. & Cuq E. (2005) Spatial and temporal variability in *Nothofagus pumilio* growth at tree line along its latitudinal range (35°40′ to 55° S) in the Chilean Andes. *J. Biogeogr.* **32,** 879–93.

LaMarche V. C., Holmes R. L., Donwiddie P. & Drew L. (1979) *Tree-Ring Chronologies Of The Southern Hemisphere: 1. Argentina. Chronology Series V*, Vol. **1**. University of Arizona, Tucson.

LeQuesne C., Aravena J. C., Alvarez-García M. A. & Fernandez-Priento J. A. (2000) Dendrocronología de *Austrocedrus chilensis* (Cupressaceae) en Chile Central. In: *Dendrocronologia en América Latina* (ed. F. Roig) pp. 159–215. EDIUNC, Mendoza.

Le-Quesne C., Acuña C., Boninsegna J. A., Rivera A. & Barichivich J. (2009) Long-term glacier variability in the Central Andes of Argentina and Chile, inferred from historical records and tree-ring reconstructed precipitation. *Palaeogeogr. Palaeoclimatol. Palaeoecol.* **281,** 334–44.

Le-Quesne C., Stahle D., Cleaveland M., Therrell M., Aravena J. C. & Barichivich J. (2006) Ancient Austrocedrus tree-ring chronologies used to reconstruct Central Chile precipitation variability from A.D. 1200 to 2000. *J. Climate* **19,** 5731–44.

Liu Y. Y., Dorigo W. A., Parinussa R. M. *et al*. (2012) Trend-preserving blending of passive and active microwave soil moisture retrievals. *Remote Sens. Environ.* **123,** 280–97. doi:10.1016/j.rse.2012.03.014.

Masiokas M. H., Villalba R., Luckman B., Delgado S., Lascano M. & Stepanek P. (2008) 20th-century glacier recession and regional hydroclimatic changes in northwestern Patagonia. *Global Planet. Change* **60,** 85–100.

Meko D. M., Touchan R. & Anchukaitis K. J. (2011) Seascorr: a MATLAB program for identifying the seasonal climate signal in an annual tree-ring time series. *Comput. Geosci.* **37,** 1234–41.

Mundo I., Roig F., Villalba R., Kitzberger T. & Barrera M. (2011) *Araucaria aracana* tree-ring chronologies in Argentina: spatial growth variations and climate influences. *Trees* **26,** 443–58.

Mundo I. A., Masiokas M. H., Villalba R. *et al*. (2012) Multi-century tree-ring based reconstruction of the Neuquen River streamflow, northern Patagonia, Argentina. *Clim. Past* **8,** 815–29.

Rebel K. T., de Jeu R. A. M., Ciais P. *et al*. (2012) A global analysis of soil moisture derived from satellite observations and a land surface model. *Hydrol. Earth Syst. Sci.* **16,** 833–47.

Rossi S., Deslauriers A., Anfodillo T. *et al*. (2006) Conifers in cold environments synchronize maximum growth rate of tree-ring formation with day length. *New Phytol.* **370,** 301–10.

Schulze E. D., Mooney H. A., Sala O. E. *et al*. (1996) Rooting depth, water availability, and vegetation cover along an aridity gradient in Patagonia. *Oecologia* **108,** 503–11.

Vaganov E. A., Hughes M. K. & Shashkin A. V. (2006) *Growth Dynamics of Conifer Tree Rings, Images of Past and Future Environments*. Springer, Berlin, Heidelberg, New York.

van der Schrier G., Barichivich J., Briffa K. & Jones P. (2013) A scPDSI-based global dataset of dry and wet spells for 1901-2009. *J. Geophys. Res.: Atmos.* doi: 10.1002/jgrd.50355.

Veblen T. T. (2007) Temperate forests of the southern Andean region. In: *The Physical Geography of South America* (eds T. T. Veblen, K. R. Young & A. R. Orme) pp. 217–31. Oxford University Press, Oxford.

Veblen T. T., Burns B. R., Kitzberger T., Lara A. & Villalba R. (1995) The ecology of the conifers of southern South America. In: *Ecology of the Southern Conifers* (eds N. J. Enright & R. S. Hill) pp. 120–55. Melbourne University Press, Melbourne.

Veblen T. T., Kitzberger T., Raffaele E. *et al*. (2008) The historical range of variability of fires in the Andean–Patagonian *Nothofagus* forest region. *Int. J. Wildland Fire* **17,** 724–41.

doi:10.1111/aec.12054

Villagran C. (2001) A model for the history of vegetation of the Coastal Range ?of central-southern Chile: Darwin's glacial hypothesis. *Rev. Chil. Hist. Nat.* **74,** 793–803.

Villalba R. (2000) Métodos en Dendrogeomorfología y su potencial uso en América del Sur. In: *Dendrocronologia en América Latina* (ed. F. Roig) pp. 103–34. EDIUNC, Mendoza.

Villalba R., Boninsegna J. & Cobos D. R. (1989) A tree-ring reconstruction of summer temperature between A.D. 1500 and 1974 in western Argentina: *Third International Conference on Southern Hemisphere Meteorology and Oceanography, Buenos Aires, Argentina, American Mateorological Society*, 196–197.

Villalba R., Cook E. R., Jacoby G. C., D'Arrigo R. D., Veblen T. T. & Jones P. D. (1998) Tree-ring based reconstructions of northern Patagonia precipitation since AD 1600. *Holoceno* **8,** 659–74.

Villalba R., D'Arrigo R. D., Cook E. R., Jacoby G. C. & Wiles G. (2001) Decadal-scale climatic variability along the extratropical western coast of the americas: evidence from tree-ring records. In: *Interhemispheric Climate Linkaje* (ed. V. Markgraf) pp. 155–70. University of Colorado, Boulder.

Villalba R., Lara A., Boninsegna J. *et al*. (2003) Large-scale temperature changes across the Southern Andes: 20th-century variability in the context of the past 400 years. *Clim. Change* **59,** 177–232.

Villalba R., Lara A., Masiokas M. H. *et al*. (2012) Unusual Southern Hemisphere tree growth patterns induced by changes in the Southern Annular Mode. *Nat. Geosci.* **5,** 793–8.

Villalba R., Masiokas M., Kitzberger T. & Boninsegna J. (2005) Biogeographical consequences of recent climate changes in the Southern Andes of Argentina. In: *Global Change and Mountain Region: An Overview of Current Knowledge* (eds U. Huber, H. K. M. Bugmann & M. A. Reasoner) p. 650. Series Advances in Global Change Research, Springer, New York.

Villalba R. & Veblen T. (1997) Spatial and temporal variability in Austrocedrus growth along the forest.steppe ecotone in northern Patagonia. *Can. J. For. Res.* **27,** 580–97.

Zhao M. & Running S.W. (2010) Drought-induced reduction in global terrestrial net primary production from 2000 through 2009. *Science* **329,** 940–3.

Zhao M. S., Heinsch F. A., Nemani R. R. & Running S. W. (2005) Improvements of the MODIS terrestrial gross and net primary production global data set. *Remote Sens. Environ.* **95,** 164–79.

SUPPORTING INFORMATION

Additional Supporting Information may be found in the online version of this article at the publisher's web-site:

Appendix S1. Summary of methods.
Appendix S2. Intercorrelation between the 21 tree-ring chronologies in the network.
Appendix S3. Correlation between tree-ring chronology and averaged precipitation and temperature.
Appendix S4. Correlation between tree-ring chronology and Jan precipitation and Feb temperature of previous year.
Appendix S5. Comparison between amplitude of the first two EOFs of the tree-ring network and the best correlated monthly or seasonal series of regional temperature and precipitation.
Appendix S6. Comparison between first EOFs based on the full network from 1750 to 1974 and on a subset of chronologies from the western Andes from 1750 to 2000.
Appendix S7. Correlations between six updated tree-ring chronologies and regional monthly soil moisture.
Appendix S8. Correlations of regionally averaged summer surface soil moisture with regional precipitation and temperature.

doi:10.1111/aec.12054

APPENDIX S1. SUPPLEMETARY MATERIAL

1) Tree-ring measurements from sixteen sites collected by LaMarche et al. (1979) and Villalba et al. (1989) were obtained from the International Tree-Ring Data Bank (ITRDB; www.ncdc.noaa.gov/paleo/treering.html). Most of these tree-ring measurements end in the 1970s and 1980s. Five new tree-ring sites were collected for this study between 2000 and 2007 in the Coastal Range of Chile and the western slope of the Andes. In addition, one site (PAG) previously collected by LaMarche et al. (1979) was updated until 2009. Most sites of this database have been used in previous studies (e.g., Holmes et al. 1979; Gonzalez and Veblen 2006; Villalba et al. 2012) but they have not yet been comprehensively analysed together.

2) Mean tree-ring chronologies for each site were developed following standard dendrochronological procedures. First, cross-dating of each core was conducted visually and validated statistically using the COFECHA Fortran routine (Holmes 1983). Then the individual growth series were detrended and standardised into relative tree-ring indices with the ARSTAN routine (Cook and Holmes 1996) by using a fixed cubic smoothing spline of 20 years to remove low-frequency variability and conserve interannual to decadal variability in the detrended series. The resulting series were then averaged together to produce a mean site chronology, which is commonly referred to as standard chronology. We refrained from analysing the multidecadal to centennial time-scale tree-ring variability because it would require the use of standardisation methods that demand larger sample sizes in order to reduce statistical and sampling biases (Briffa and Melvin 2011). Such a task will be addressed in a future study.

3) The Expressed Population Signal statistic measures the degree of the common variability between tree-ring series in a given site and period taking into account sample replication. EPS was computed with the ARSTAN routine using 50-year sliding windows with 25 years of overlap.

4) The mean sensitivity (MS) ranges from 0 to 1 and is simply the mean relative difference in annual growth from one year to the next, thereby integrating the temporal carry-over (serial correlation) and interannual variability (standard deviation) of tree-ring width. Hence, high MS indicates more variable radial growth and typically higher values occur in regions with stronger environmental variability such as arid and semiarid regions (Fritts 1976).

5) The soil moisture dataset is based on the statistical blending of passive (SMMR: November 1978-August 1987; SSM/I: July 1987-2007; TMI: 1998-2008 and AMSR-E: July 2002-2010) and active (ERS-1/2: July 1991-May 2006 and ASCAT: 2007-2010) satellite microwave observations since November 1978, which preserves the long-term variability and minimises temporal inhomogeneities due to changing satellite sensors (Liu et al. 2012; Dorigo et al. 2012).

6) Because there are no moisture observations under snow conditions, the daily data at each grid point were aggregated to monthly averages during the warm season (October to March) and then a summer soil moisture series was computed for the study region as done above for temperature and precipitation. Prior to analysis, the monthly and summer soil moisture series were linearly detrended over their full length in order to minimise the influence of a potential discontinuity in the early part of the dataset due to the merging of the SMMR (1978-1987) and SSM/I (1987-2007) sensors based on a very short overlap. Then, detrended grid-level and regionally averaged summer soil moisture was correlated with the first EOF of the six updated chronologies over the period 1979-2000. In addition, each of the six chronologies was correlated with monthly regional soil moisture during the current and previous warm seasons (October to March) in order to identify the critical months when soil moisture limits tree growth. Grid points with less than 15 years of observations were excluded from analysis.

7) The number of sites with significant correlations in January drops to six when using partial instead of simple correlations, but the main pattern remains (Figure S2A in the auxiliary material). The strength of the correlations between tree rings and precipitation during this month does not vary significantly ($p < 0.05$) along any gradient in elevation, latitude or longitude (Figure S3A in the auxiliary material).

8) There is also a consistent but not significant pattern of positive correlation with late-winter and early spring temperatures (August-October; partial $r = 0.16$ to 0.25, $p > 0.05$) during the previous and current growing seasons. As noted above, this positive relationship with spring temperatures is significant in some sites and may be related to a dominant limitation of cambial activity and tree-ring growth by low temperatures at this time of the year.

9) Overall, simple and partial correlations with regional monthly temperature and precipitation highlight the lagged character of the response of Araucaria tree-ring growth to climate variability, with a changing but predominantly negative influence of temperature through the previous growing season and a relatively weaker but still significant response to precipitation during the peak of the growing season. These general patterns of correlation are not sensitive to the use of simple or partial correlations (Figure S2 in the auxiliary material) and appear to vary only along the longitudinal moisture gradient (Figure S3 in the auxiliary material). Taken together, these results suggest a dominant control of tree-ring growth by moisture availability that becomes stronger toward the driest part of the moisture gradient in the eastern side of the Andes.

REFERENCES

Briffa K. & Melvin T. M. (2011) A closer look at regional curve standardization of tree-ring records: justification of the need, a warning of some pitfalls, and suggested improvements in its application. In: *Dendroclimatology: Progress and Prospects* (eds M. K. Hughes *et al.*) pp. 113–46. Springer, Dordrecht.

Cook E. R. & Holmes R. L. (1996) *Users Manual for Program ARSTAN*. University of Arizona, Tucson.

Holmes R. L. (1983) Computer-assisted quality control in tree-ring dating and measurement. *Tree-Ring Bulletin* **44**, 69–75.

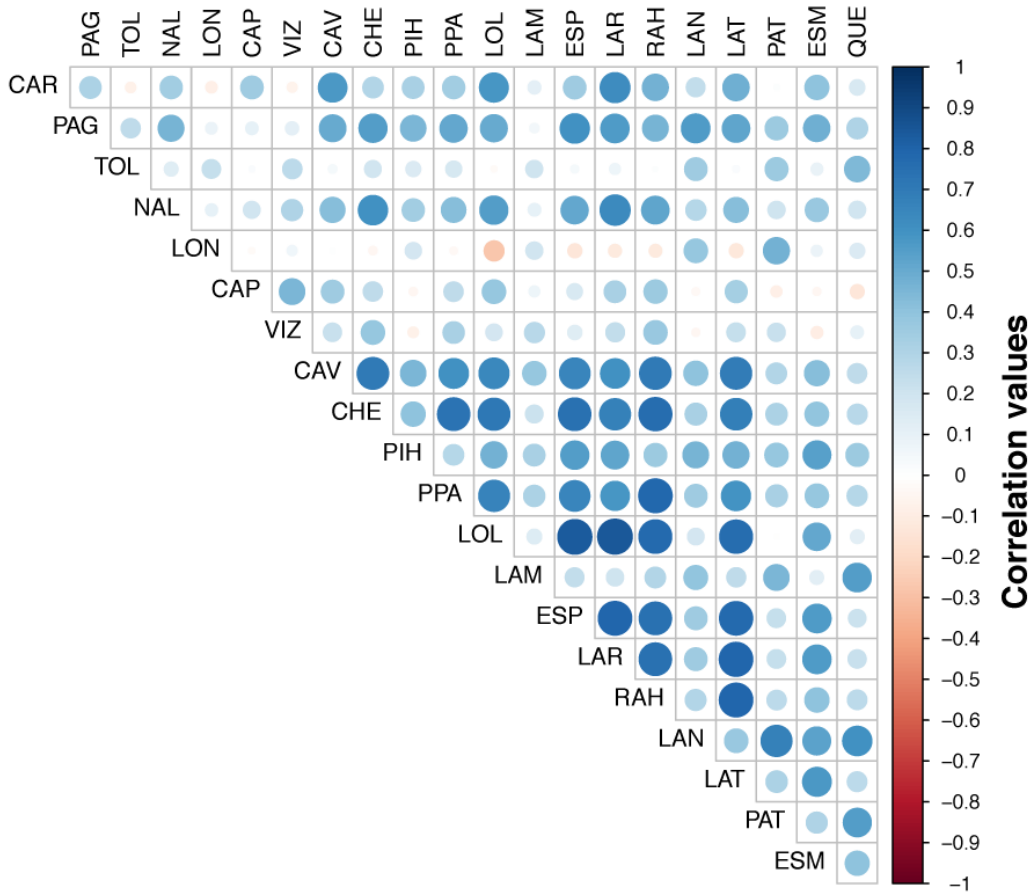

Appendix S2. Intercorrelation between the 21 tree-ring chronologies in the network.

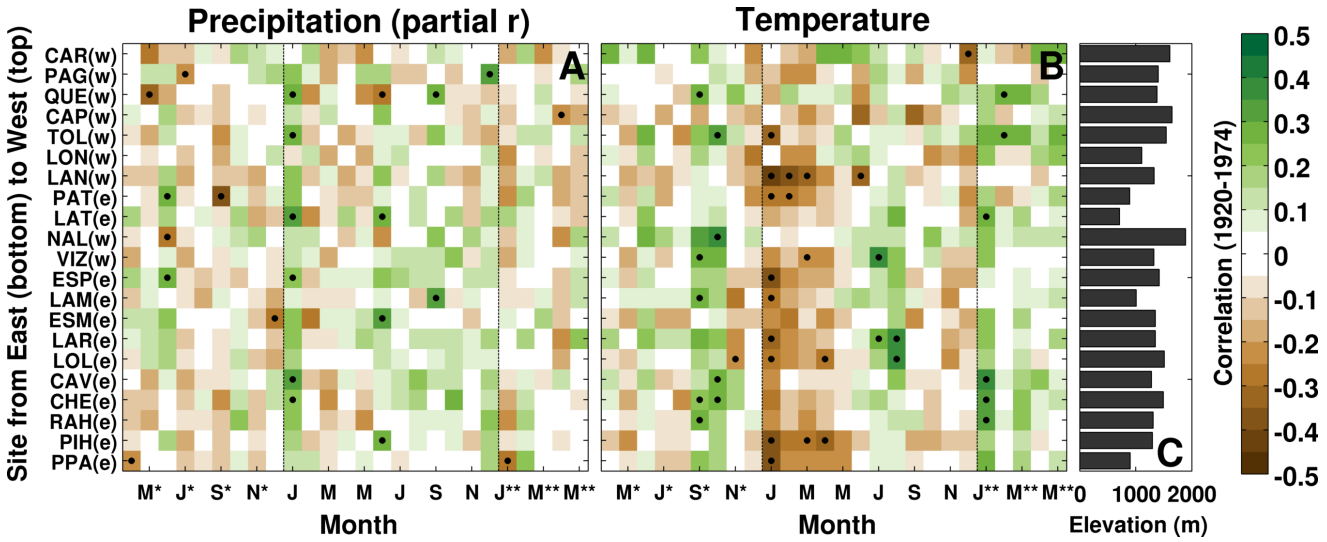

Appendix S3. Correlation between each tree-ring chronology in the network and regionally averaged (A) total monthly precipitation and (B) mean monthly temperature within a 26-month window from April of the previous calendar year (*) to May of the following year (**) during 1920–1974. Partial correlations are given for precipitation and simple correlation for temperature. The stippling indicates months with significant correlations ($p < 0.05$). The elevation of the chronologies is shown in C and their location east (e) or west (w) of the continental divide is given next to the site name.

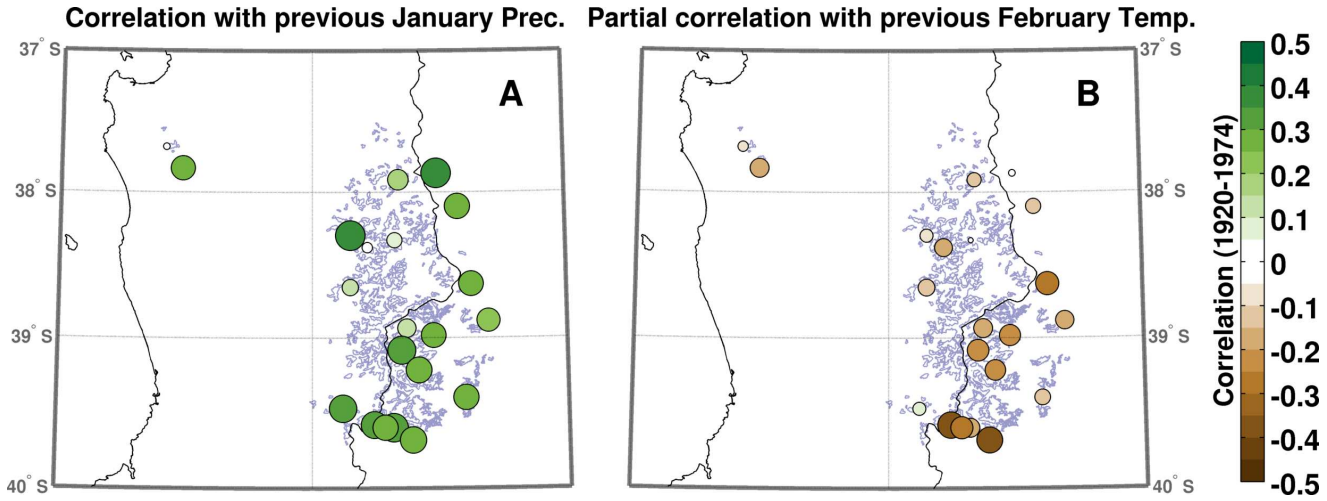

Appendix S4. Correlation between the individual tree-ring chronologies and (A) January precipitation and (B) February temperatures during the previous growing season from 1920 to 1974. Note that partial correlations are shown for temperature. The size and colour of the markers are proportional to the magnitude of the correlations.

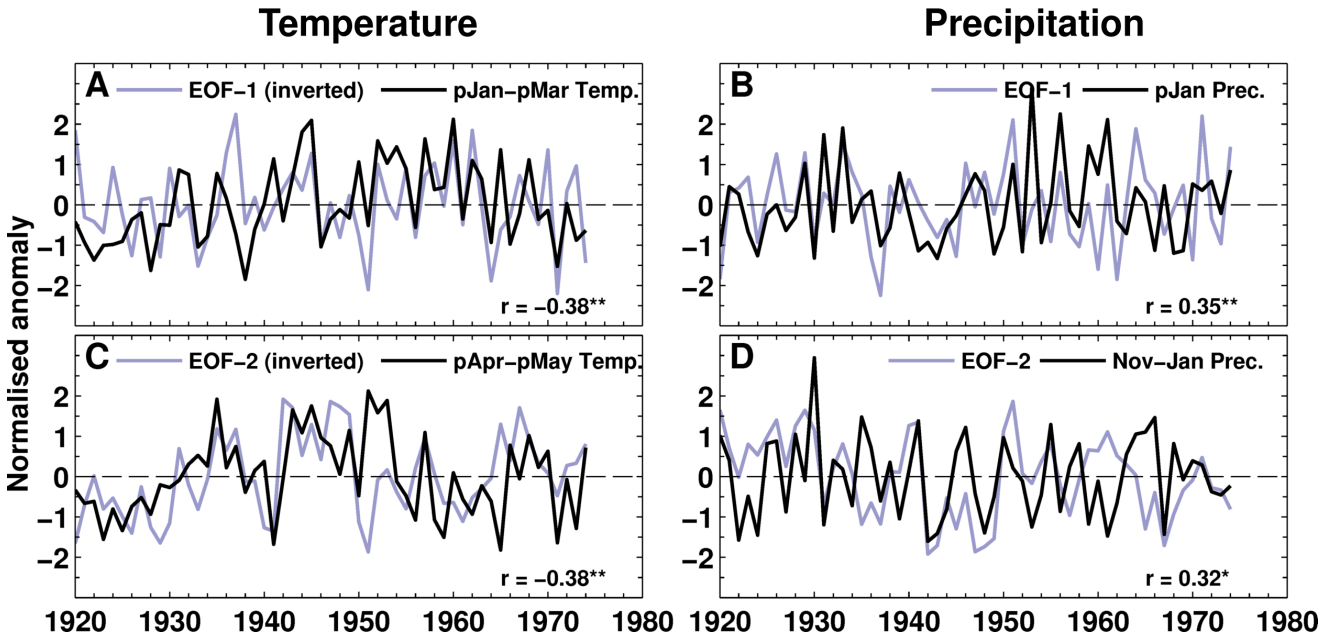

Appendix S5. Comparison between the amplitude of the first two EOFs of the tree-ring network and the best correlated monthly or seasonal series of regional (A, C) temperature and (B, D) precipitation from 1920 to 1974. The simple correlation coefficient between the series is given in each panel. An asterisk indicates significant correlations (* for $p < 0.05$ and ** for $p < 0.01$). Months prior to the start of the austral growing season in September of the current calendar year are indicated by the prefix p.

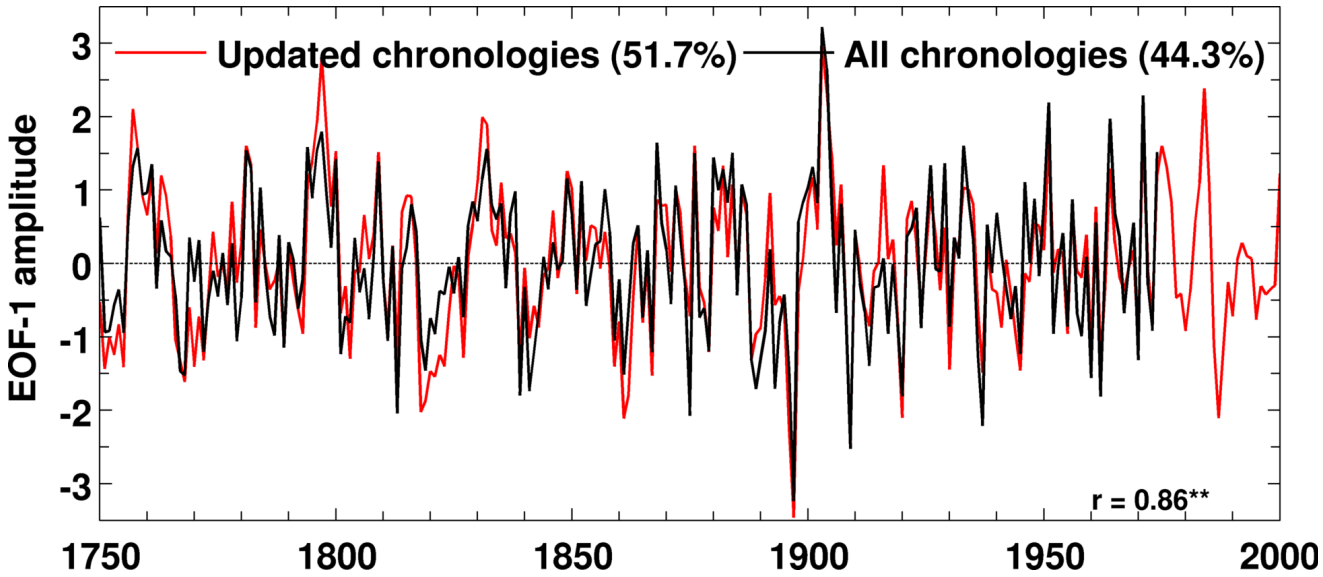

Appendix S6. Comparison between the first EOF based on the full network over the period 1750-1974 and the first EOF based on a subset of six chronologies in the western side of the Andes covering the period 1750–2000. The two series are highly correlated ($p < 0.01$), indicating that the EOF of the updated chronologies captures the regional growth signal seen in the entire network.

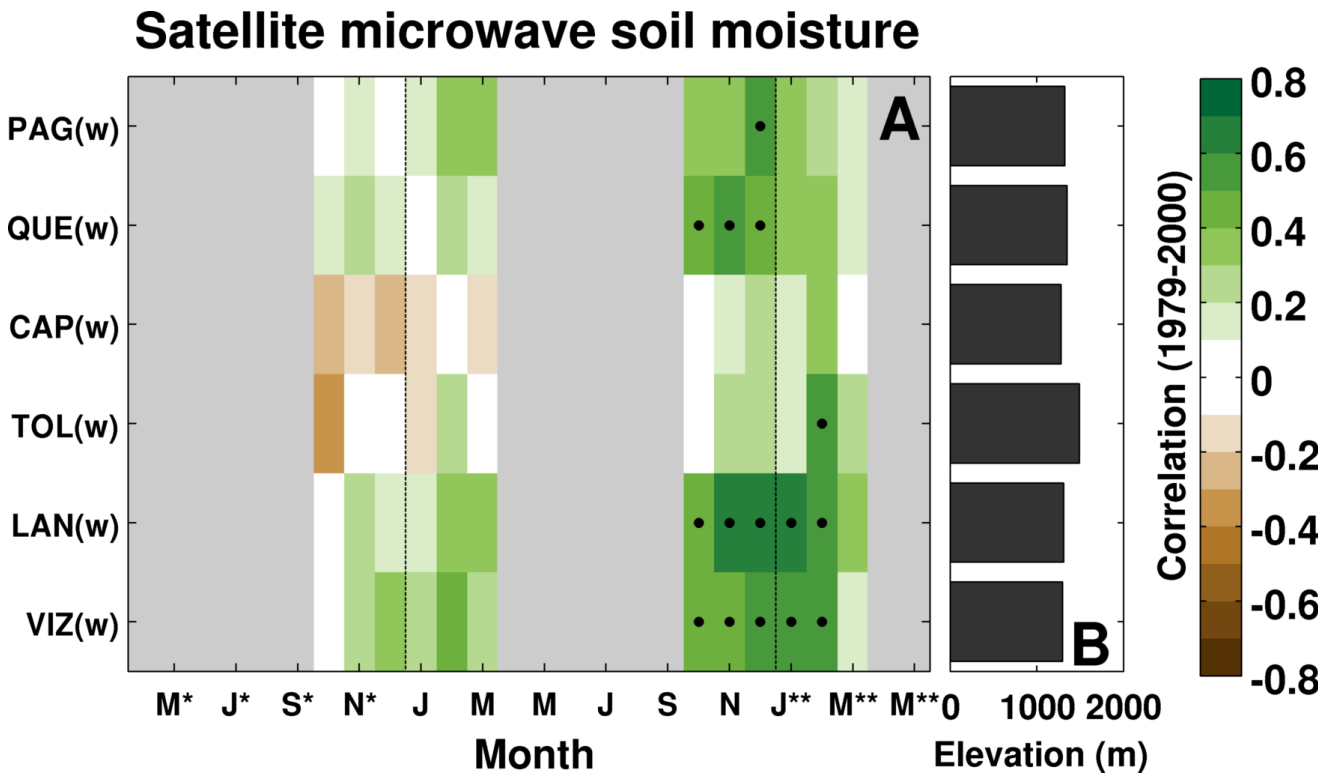

Appendix S7. Correlation between the six updated tree-ring chronologies and regional monthly satellite-observed soil moisture during the previous and current growing seasons from 1979 to 2000. The stippling indicates months with significant correlations ($p < 0.05$). The elevation of the chronologies is shown in C and their location east (e) or west (w) of the continental divide is given next to the site name. The satellite observations reveal a statistically significant response to spring and summer surface soil moisture during the current growing season in most of the sites.

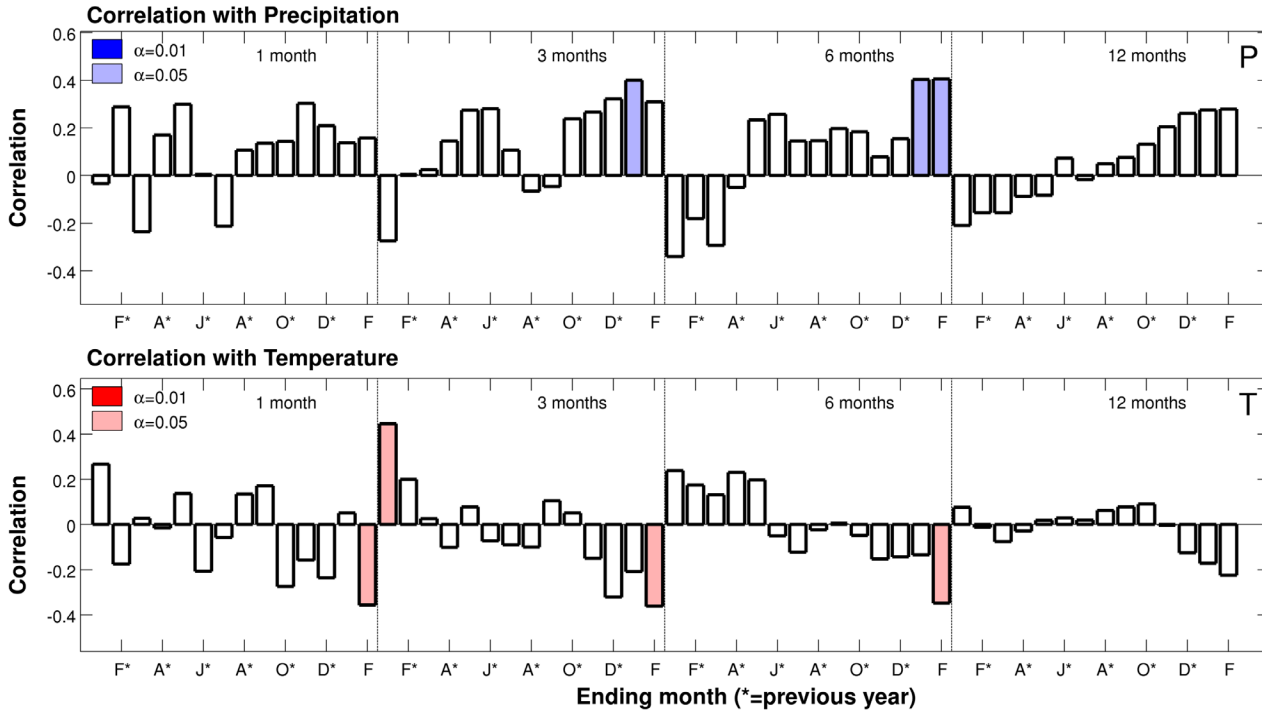

Appendix S8. Correlation of regionally averaged summer (December-February) satellite-observed surface soil moisture with monthly, 3-month, 6-month, 9-month and 12-month aggregated regional precipitation (top) and temperature (bottom) over the period 1980–2010. Correlations are given for a 14-month temporal window from January of the previous year to February of the current year.